

Energy-dependent multipole analysis for photoproduction of pions from neutrons

Alexander W. Smith and N. Zagury

Departamento de Física, Pontifícia Universidade Católica, Cx.P. 38071, Rio de Janeiro, RJ, Brasil

(Received 17 September 1979)

An energy-dependent multipole analysis for photoproduction of pions from neutrons from threshold up to 450 MeV is presented.

I. INTRODUCTION

In a recent article¹ we made a multipole analysis of photoproduction of pions off protons from threshold up to photon laboratory energy equal to 450 MeV. In this article we extend our analysis to photoproduction of pions from neutrons.

The experimental results for photoproduction of pions from neutrons are in much poorer shape than in the case of protons. The main reason is that a pure neutron target does not exist, and the results have to be extracted from deuteron measurements. This implies several uncertainties due to the particular models used in the extraction of the results. Also the number of experimental results available is much less than in the case of proton targets. For example, in the region of photon laboratory energies (K_L) from threshold up to 450 MeV there is no report, in the recent data compilation of Menze, Pfeil, and Wilcke,² of nucleon-recoil polarization measurements and just one result for a polarized-target experiment.

Dispersion-relation techniques have provided a useful tool for the description of photoproduction of pions. In fact, this approach has successfully given a good understanding of photoproduction of pions in protons in the region of the first resonance³ and should provide a first approximation for our multipole analysis.

In this article we assume that the $j > \frac{3}{2}$ multipoles are given by the Born terms and try to determine the other multipoles using as a first approximation a dispersion-relations model and correcting it by the product of three terms: (a) a phase factor as given by the Fermi-Watson theorem,⁴ (b) threshold-behavior dependence, (c) a second-degree polynomial in energy (three adjustable parameters for each multipole).

In Sec. II we make some general considerations and in Sec. III we present our results.

II. GENERAL CONSIDERATIONS

If we assume that the electromagnetic current transforms like the sum of an isoscalar and an isovector, the four reactions $\gamma + N \rightarrow \pi + N$ can be

described in terms of three independent isospin amplitudes. These transition amplitudes will be called T^S , T^{V1} , and T^{V3} and correspond to the isoscalar amplitude, the $I = \frac{1}{2} \rightarrow I = \frac{1}{2}$ and the $I = \frac{1}{2} \rightarrow I = \frac{3}{2}$ isovector transition amplitudes. The T matrix for the four reactions $\gamma + N \rightarrow \pi + N$ may be written as

$$\begin{aligned} \langle \pi^+ n | T | \gamma p \rangle &= \sqrt{2} (T^S + T^{V1}/3 - T^{V3}/3), \\ \langle \pi^0 p | T | \gamma p \rangle &= T^S + T^{V1}/3 + 2T^{V3}/3, \\ \langle \pi^0 n | T | \gamma n \rangle &= -T^S + T^{V1}/3 + 2T^{V3}/3, \\ \langle \pi^- p | T | \gamma n \rangle &= \sqrt{2} (T^S - T^{V1}/3 + T^{V3}/3). \end{aligned} \quad (2.1)$$

The existence of an isotensor component in the electromagnetic current would mean that the four amplitudes in the left-hand side of Eqs. (2.1) are independent.

As usual we denote by $M_{i\pm}^I$ and $E_{i\pm}^I$ the magnetic and electric multipoles leading to final isotopic spin I , orbital angular momentum l , and total angular momentum $j = l \pm \frac{1}{2}$. In what follows we will use the generic symbol $h_{i\pm}^I$ to denote either $M_{i\pm}^I$ or $E_{i\pm}^I$.

As in Ref. 1 we assume that all $h_{i\pm}^I$ are given by the sum of two terms: $h_{i\pm}^I(\text{input})$ and an adjustable correction $\Delta h_{i\pm}^I$. For all nonresonant amplitudes $h_{i\pm}^I(\text{input})$ is given by the Born term corrected for absorption⁵:

$$h_{i\pm}(\text{input}) = (\text{Born approx}) \times \exp(i\delta_{i\pm}^I) \cos\delta_{i\pm}^I, \quad (2.2)$$

where $\delta_{i\pm}^I$ is the phase shift for πN scattering in the channel $(I, j = l \pm \frac{1}{2})$. The resonant $h_{i\pm}^{3/2}(\text{input})$ is taken from Chew, Goldberger, Low, and Nambu⁶ dispersion-relation results:

$$\begin{aligned} E_{1+}^{3/2}(\text{input}) &= 0, \\ M_{1+}^{3/2}(\text{input}) &= \frac{\mu_p - \mu_n}{2} \frac{m_\pi}{f^2} \frac{k}{q^2} \end{aligned} \quad (2.3)$$

$$\times \exp(i\delta_{1+}^{3/2}) \sin\delta_{1+}^{3/2},$$

where $f^2 = 0.08$ and μ_p and μ_n are the magnetic moments for proton and neutron and k and q are the photon and pion momentum in the center-of-mass system.

The correction for the $j \leq \frac{3}{2}$ multipoles are

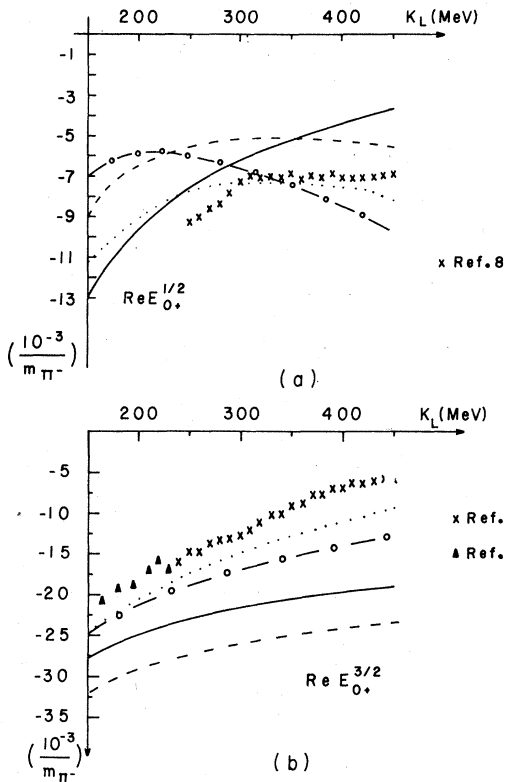


FIG. 1. (a) The real part of $E_{0+}^{1/2}$; (b) the real part of $E_{0+}^{3/2}$. The solid line is the input. The dotted line, the —○— line, and the dashed line correspond to solutions A, B, and C, respectively.

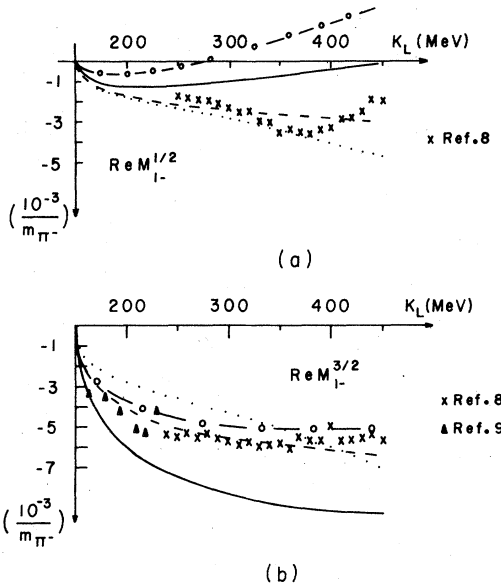


FIG. 2. (a) The real part of $M_{1-}^{1/2}$; (b) the real part of $M_{1-}^{3/2}$. The convention for the lines is the same as in Fig. 1.

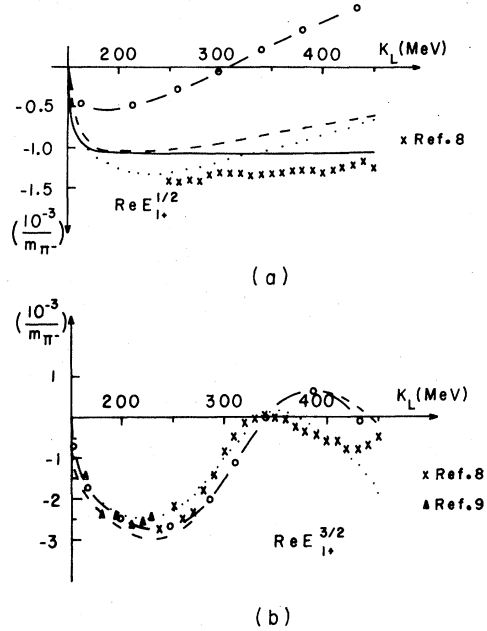


FIG. 3. (a) The real part of $E_{1+}^{1/2}$; (b) the real part of $E_{1+}^{3/2}$. The convention for the lines is the same as in Fig. 1. For $E_{1+}^{3/2}$ the input is zero.

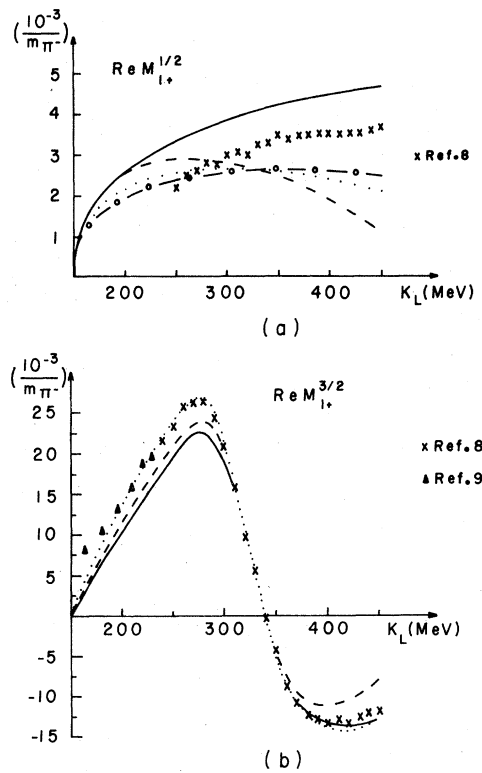


FIG. 4. (a) The real part of $M_{1+}^{1/2}$; (b) the real part of $M_{1+}^{3/2}$. The convention for the lines is the same as in Fig. 1. For $M_{1+}^{3/2}$ the difference between solutions A and B is negligible and is not shown in the figure.

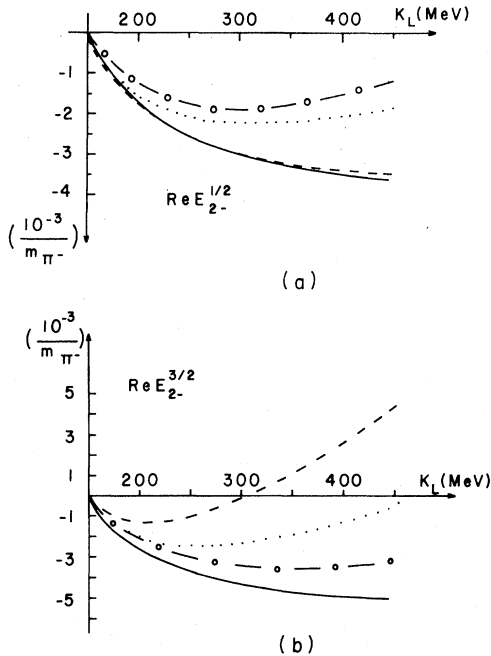


FIG. 5. (a) The real part of $E_{2-}^{1/2}$; (b) the real part of $E_{2-}^{3/2}$. The convention for the lines is the same as in Fig. 1.

taken as

$$\Delta h_{i\pm}^i = \exp(i\delta_{i\pm}^i) q^i (a_{i\pm}^i + b_{i\pm}^i W + c_{i\pm}^i W^2), \quad (2.4)$$

where $\exp(i\delta_{i\pm}^i)$ assures the correct phase as given by the Fermi-Watson theorem,⁴ q^i assures the correct threshold behavior, W is the total energy in the center-of-mass system, and $a_{i\pm}^i$, $b_{i\pm}^i$, and $c_{i\pm}^i$ are adjustable parameters. These parameters have been determined by searching for the minimum of the χ_ω^2 function defined as

$$\chi_\omega^2 = \frac{1}{N-n} \sum_{i=1}^N \omega_i \left(\frac{y_{\text{expt}}^i - y_{\text{calc}}^i}{\Delta y_{\text{expt}}^i} \right)^2, \quad (2.5)$$

where N is the total number of events, n is the number of parameters in the fit, y_{expt}^i , Δy_{expt}^i , and y_{calc}^i are the experimental value, the corresponding experimental error and the calculated value of the measurable quantities at a given angle and energy; ω_i is a weight factor that will be defined in the next section.

III. RESULTS

The experimental results were taken from Menze, Pfeil, and Wilcke's data collection² and the π - N phase shifts from Almehed and Lovelace's⁷ analysis. The experimental data for photoproduction from neutrons is quite poor, mainly for π^0 production where we have only few events listed for the differential cross section and

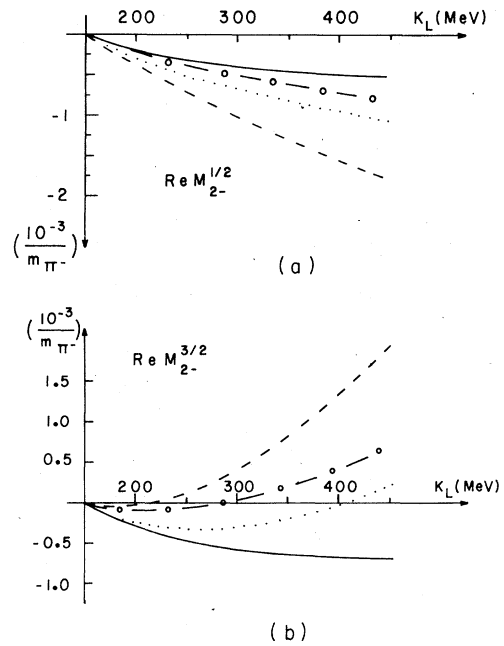


FIG. 6. (a) The real part of $M_{2-}^{1/2}$; (b) the real part of $M_{2-}^{3/2}$. The convention for the lines is the same as in Fig. 1.

for the $\pi^0 n / \pi^0 p$ ratio in deuteron experiments. These two kinds of data were collapsed together by generating the $\gamma + n \rightarrow \pi^0 + n$ cross section from the $\pi^0 n / \pi^0 p$ ratio times our previous results¹ for the differential cross section for $\gamma + p \rightarrow \pi^0 + p$. Although the number of π^- events is larger, there is just one event listed for polarized-target asymmetry and none for final-nucleon polarization. These last two quantities measure the interference between the real and imaginary parts of the amplitudes and are quite important for the determination of the small multipoles, in the resonance region.

We first try to determine the multipoles by looking for the minimum of χ_ω^2 using the neutron data alone, $\omega_i = 1$ and taking $h_{i\pm}^{3/2}$ as known and equal to solution A of our previous proton fit.¹

TABLE I. Distribution of data used in the fits. $\sigma(\theta)$ is the differential cross section, $P(\theta)$ is the final-nucleon polarization, $T(\theta)$ is the polarized-target asymmetry, and $\Sigma(\theta)$ is the polarized-photon asymmetry.

	$\sigma(\theta)$	$P(\theta)$	$T(\theta)$	$\Sigma(\theta)$
$\gamma + n \rightarrow \pi^- + p$	501	0	1	68
$\gamma + n \rightarrow \pi^0 + n$	70	0	0	0
$\gamma + p \rightarrow \pi^+ + n$	1218	7	23	139
$\gamma + p \rightarrow \pi^0 + p$	757	26	9	72

TABLE II. Multipoles for solution A. K_L is given in MeV and the multipoles in units of $10^{-3}/m_{\pi^-}$.

K_L	$E_{0+}^{1/2}$	$M_{1-}^{1/2}$	$E_{1+}^{1/2}$	$M_{1+}^{1/2}$	$E_{2-}^{1/2}$	$M_{2-}^{1/2}$	$E_{0+}^{3/2}$	$M_{1-}^{3/2}$	$E_{1+}^{3/2}$	$M_{1+}^{3/2}$	$E_{2-}^{3/2}$	$M_{2-}^{3/2}$
160	-10.80	-1.06	-0.86	1.28	-0.59	-0.10	-24.04	-1.62	-1.52	1.89	-0.79	-0.09
170	-10.25	-1.32	-1.03	1.59	-0.89	-0.15	-23.05	-2.03	-1.88	6.75	-1.19	-0.15
180	-9.78	-1.52	-1.13	1.83	-1.15	-0.21	-22.12	-2.33	-2.12	9.17	-1.51	-0.19
190	-9.39	-1.69	-1.20	2.01	-1.36	-0.26	-21.31	-2.57	-2.29	11.28	-1.76	-0.23
200	-9.10	-1.83	-1.24	2.15	-1.54	-0.30	-20.54	-2.78	-2.39	12.99	-1.96	-0.26
210	-8.74	-1.96	-1.26	2.27	-1.68	-0.35	-19.84	-2.96	-2.45	14.51	-2.12	-0.28
220	-8.42	-2.07	-1.27	2.37	-1.80	-0.39	-19.16	-3.13	-2.46	17.11	-2.23	-0.30
230	-8.16	-2.18	-1.28	2.45	-1.91	-0.43	-18.52	-3.28	-2.43	19.36	-2.31	-0.31
240	-8.03	-2.28	-1.27	2.51	-1.99	-0.47	-17.91	-3.43	-2.35	21.25	-2.36	-0.32
250	-7.81	-2.39	-1.27	2.56	-2.06	-0.51	-17.36	-3.57	-2.24	22.80	-2.39	-0.33
260	-7.62	-2.49	-1.25	2.60	-2.11	-0.54	-16.82	-3.71	-2.08	24.25	-2.40	-0.33
270	-7.54	-2.59	-1.23	2.62	-2.15	-0.58	-16.29	-3.85	-1.85	25.47	-2.39	-0.33
280	-7.49	-2.69	-1.21	2.64	-2.19	-0.61	-15.79	-3.99	-1.58	25.39	-2.36	-0.32
290	-7.40	-2.79	-1.19	2.66	-2.21	-0.64	-15.32	-4.14	-1.29	23.88	-2.31	-0.31
300	-7.46	-2.90	-1.17	2.66	-2.22	-0.67	-14.85	-4.28	-0.95	20.54	-2.25	-0.30
310	-7.38	-3.01	-1.14	2.66	-2.23	-0.70	-14.41	-4.43	-0.64	15.89	-2.18	-0.28
320	-7.35	-3.11	-1.11	2.65	-2.23	-0.73	-13.96	-4.59	-0.37	10.78	-2.11	-0.26
330	-7.40	-3.23	-1.08	2.64	-2.22	-0.76	-13.54	-4.74	-0.16	5.60	-2.02	-0.24
340	-7.41	-3.34	-1.05	2.62	-2.21	-0.79	-13.14	-4.91	-0.04	1.72	-1.92	-0.22
350	-7.41	-3.46	-1.02	2.59	-2.20	-0.82	-12.75	-5.07	0.09	-5.19	-1.81	-0.19
360	-7.35	-3.58	-0.99	2.56	-2.18	-0.85	-12.40	-5.25	0.08	-8.28	-1.70	-0.16
370	-7.42	-3.69	-0.95	2.53	-2.16	-0.87	-11.98	-5.43	0.02	-10.80	-1.58	-0.13
380	-7.56	-3.80	-0.92	2.50	-2.13	-0.90	-11.62	-5.59	-0.11	-12.37	-1.46	-0.09
390	-7.64	-3.93	-0.89	2.46	-2.10	-0.93	-11.28	-5.77	-0.29	-13.16	-1.33	-0.06
400	-7.57	-4.04	-0.85	2.40	-2.06	-0.95	-10.93	-6.00	-0.50	-13.31	-1.19	-0.02
410	-7.59	-4.18	-0.81	2.35	-2.03	-0.97	-10.61	-6.20	-0.74	-13.29	-1.05	0.03
420	-7.62	-4.32	-0.78	2.31	-2.00	-1.00	-10.30	-6.41	-1.01	-13.05	-0.91	0.07
430	-7.73	-4.45	-0.74	2.26	-1.96	-1.02	-9.99	-6.63	-1.30	-12.65	-0.76	0.12
440	-7.92	-4.57	-0.70	2.20	-1.91	-1.05	-9.67	-6.85	-1.62	-12.15	-0.61	0.17
450	-8.19	-4.65	-0.66	2.14	-1.86	-1.07	-9.33	-7.08	-1.95	-11.56	-0.46	0.22

Therefore we will have to find eighteen parameters a , b , and c corresponding to six multipoles with $j \leq \frac{3}{2}$ and final isotopic spin $I = \frac{1}{2}$ corresponding to the combination $T^S + T^{V1}/3$ of the T matrix. This solution A is the one in which we have more confidence.

We have analyzed the data in two other different ways in order to study the influence of the neutron

data in the determination of $h_{i\pm}^{3/2}$ and in order to see if, even with such poor neutron data, the results would confirm the hypothesis of no isotensor current.

Solution B considers all neutron and proton data together. In this case we will have to find 54 parameters for the eighteen multipoles with $j \leq \frac{3}{2}$ and corresponding to the transitions T^S , T^{V1} ,

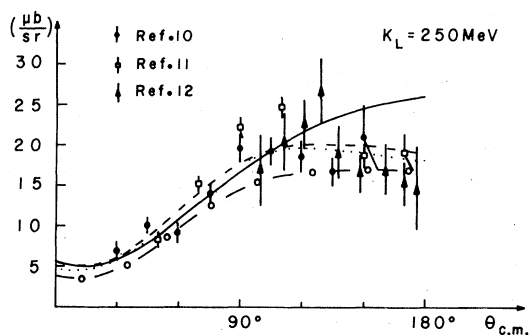


FIG. 7. Differential cross section for π^- photoproduction at 250 MeV. The convention for the lines is the same as in Fig. 1.

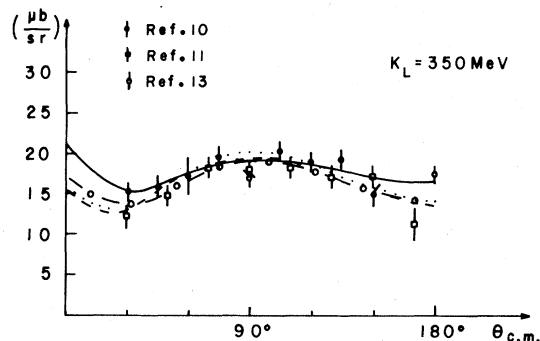


FIG. 8. Differential cross section for π^- photoproduction at 350 MeV. The convention for the lines is the same as in Fig. 1.

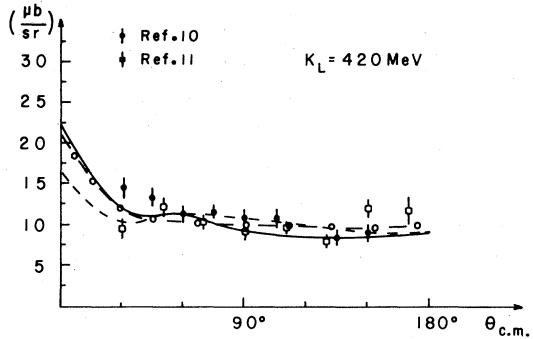


FIG. 9. Differential cross section for π^- photoproduction at 420 MeV. The convention for the lines is the same as in Fig. 1.

and T^{V3} . To balance the importance of each reaction (2.1) we set

$$\omega_i = N/2n_r^i, \quad (3.1)$$

where n_r^i is the number of events in the reaction to which the event i belongs.

Although the small number of data for final π^0 's does not justify the determination of two independent isotopic spin amplitudes from the neutron data alone, we have tried it as a check for our results. In this case, called solution C, we have 36 parameters to determine. To balance the influence of the π^0 and π^- events we use the same weight as in

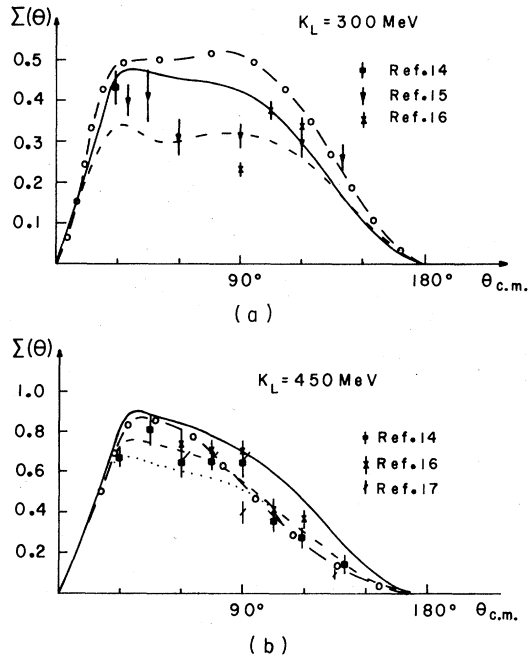


FIG. 10. Photon asymmetry for π^- photoproduction: (a) at 300 MeV; (b) at 450 MeV. The convention for the lines is the same as in Fig. 1.

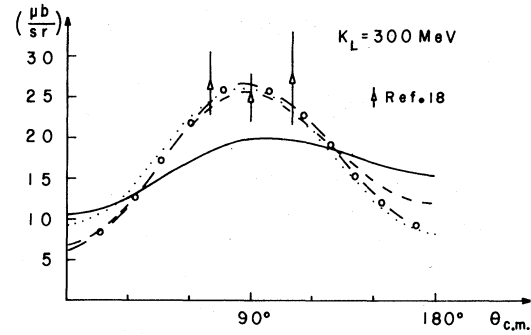


FIG. 11. Differential cross section for π^0 photoproduction at 300 MeV. The convention for the lines is the same as in Fig. 1. The experimental points correspond to $299 \leq K_L \leq 301$ MeV.

case B.

To save memory and computational time the data was divided in intervals of 5 MeV. We look for a minimum of χ_ω^2 and have obtained the values 2.71, 2.98, and 1.95 for solutions A, B, and C, respectively.

Figures 1-6 show our results for the multipoles. We notice that solutions A and B are quite close for the larger multipoles except for $E_{0+}^{1/2}$. Solutions A and B also agree reasonably well for most $I = \frac{3}{2}$ multipoles. Although solution C should not have any very deep statistical meaning, it agrees with solution A for some of the multipoles, giving more confidence in their determination. For comparison we also plot the results of Berends and Donnachie⁸ and of Berends and Weaver.⁹

As it was pointed out before, the neutron data are quite poor. The proton data used, on the other hand, are much more adequate as Table I shows. We will, therefore, consider solution A which uses the known results for T^{V3} from the proton fit¹ as our best solution, although its results should not be considered as definitive, in particular for those multipoles where solutions A and B do not agree well.

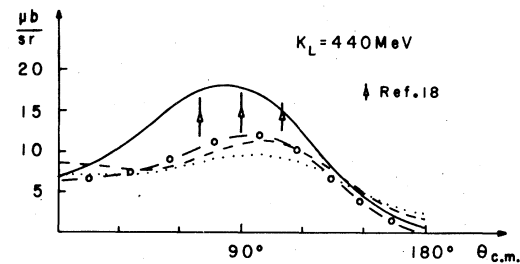


FIG. 12. Differential cross section for π^0 photoproduction at 440 MeV. The convention for the lines is the same as in Fig. 1. The experimental points correspond to $437 \leq K_L \leq 443$ MeV.

Although solution C has no bias from any previous proton fit and is independent of any hypothesis on the isospin dependence of the electromagnetic current, it is quite difficult to draw any conclusion from its results. Nevertheless, for one of the large multipoles, namely $M_{1+}^{3/2}$, solutions A and C agree reasonably well. This is not true for the two large multipoles $E_{0+}^{3/2}$ and $E_{0+}^{1/2}$. Actually these differences come mostly from the isospin combination that corresponds to final π^0 where the data is worse. We think it should be

improper to attribute these differences to the existence of an isotensor component of the electromagnetic current, for the time being. In Table II we give the numerical values for the multipoles in solution A, and in Figs. 7-10 we show how our results fit the experimental values for final π^- differential cross section at $K_L = 250, 350,$ and 420 MeV and photon asymmetry at $K_L = 300$ and 450 MeV. We also show in Figs. 11 and 12 the differential cross section for π^0 production at energies $K_L = 300$ and 440 MeV.

¹Alexander W. Smith and N. Zagury, Phys. Rev. D 20, 2719 (1979). See also J. R. Rios Leite and N. Zagury, Rev. Bras. Fis. 4, 191 (1974).

²D. Menze, W. Pfeil, and R. Wilcke, Physik Daten 7-1 (1977).

³See for example, S. Adler, Ann. Phys. (N.Y.) 50, 189 (1968).

⁴K. Watson, Phys. Rev. 95, 228 (1954); E. Fermi, Suppl. Nuovo Cimento 2, 58 (1955).

⁵See for example, Goldberger and Watson, *Collision Theory* (Wiley, New York, 1964), p. 547.

⁶G. F. Chew, M. L. Goldberger, F. E. Low, and Y. Nambu, Phys. Rev. 106, 1345 (1957).

⁷S. Almehed and C. Lovelace, Nucl. Phys. B40, 157 (1972).

⁸F. A. Berends and A. Donnachie, Nucl. Phys. B84, 342

(1975).

⁹F. A. Berends and D. L. Weaver, Nucl. Phys. B30, 575 (1971).

¹⁰T. Fujii *et al.*, Nucl. Phys. B120, 395 (1977).

¹¹P. Benz *et al.*, Nucl. Phys. B65, 158 (1973).

¹²J. Boucrot *et al.*, Nuovo Cimento A18, 635 (1973).

¹³T. Fujii *et al.*, Phys. Rev. Lett. 26, 1672 (1971).

¹⁴V. B. Ganenko *et al.*, Yad. Fiz. 19, 1245 (1974) [Sov. J. Nucl. Phys. 19, 637 (1974)].

¹⁵V. B. Ganenko *et al.*, Zh. Eksp. Teor. Fiz. Pis'ma Red. 16, 535 (1972) [JETP Lett. 16, 380 (1972)].

¹⁶K. Kondo *et al.*, Phys. Rev. D 9, 529 (1974).

¹⁷F. F. Lin *et al.*, Phys. Rev. B 136, 1183 (1964).

¹⁸A. Ando *et al.*, contribution to the International Symposium on Lepton and Photon Interactions at High Energies, Stanford University, 1975 (unpublished).